



## Artificial neural network modelling for the removal of lead from wastewater by using adsorption process

Ayat Hussein Mahdi<sup>a,\*</sup>, Ghaidaa Majeed Jaid<sup>a</sup>, Saja Mohsen Alardhi<sup>b</sup>

<sup>a</sup>Department of Civil Engineering, University of Technology, Baghdad, Iraq, email: Ayat.H.Mahdi@uotechnology.edu.iq (A.H. Mahdi), 40325@uotechnology.edu.iq (G.M. Jaid)

<sup>b</sup>Nanotechnology and Advanced Materials Research Center, University of Technology, Iraq, email: 11659@uotechnology.edu.iq

Received 6 July 2021; Accepted 25 October 2021

---

### ABSTRACT

For the current work, almond shell was used from activated carbon via the chemical activation with phosphoric acid (85%) by a weight rate of (1:1) to remove lead ion from contaminated water by a batch adsorption process. Activated carbon was characterized by XRD, EDX and SEM analysis. ANN (artificial neural network) modelling was excellent to forecast and check the removal efficiency and the impacts of operational parameters on the removal efficiency. The experimental variables for the adsorption process were utilized as input data for a neural network to train and calculate the output removal efficiency of lead. The activated carbon dosage was the most significant factor in adsorbing technique. The acquired experimentation data was fixed to the adsorbing isotherms (Langmuir and Freundlich) and Freundlich model was found to be the closest to experimental data. The removal kinetic modelling used the pseudo-first-order and pseudo-second-order, the pseudo-second-order provided the best description of the kinetic demeanor. The novelty of this work is obtained by using Almond shell in a sustainable manner by predicting the most affecting factor on removal efficiency, which is supposed to be AC dosage, using ANN model.

*Keywords:* Almond shell; Activated carbon; Batch experiments; Artificial neural network; Isotherm; Kinetic model

---

### 1. Introduction

Nowadays, with the sophisticated life system and to keep up with industrial, technological, and agricultural advancement, the rapid pace of this development has led to severe problems in the ecosystem [1]. Releasing of heavy metals into waters is due to various industry acts such as chemical industries, electroplating, mining, batteries and other industries that have led to water pollution and a serious change in the environment and human health cause these metals are toxic and non-degradable [2].

Efforts are focused on developing substitutions that are environmentally friendly for removing an extensive variety of contaminants. Various agricultural waste materials consist of lignocellulosic fibers which are effective for the

treatment of colored and wastewater contamination due to their adsorptive capacity of pollutants [3].

Activated carbon is an extremely absorbent carbon material that can be attained from agricultural waste, having a great carbon content like cellulose. The most important specification for these materials is the larger porosity and larger surface area than other conventional adsorbents. On the other hand, the features mainly depend on the material's type, exposed temperature, and conditions of activating. Better removal efficiency is attained via surface adjustments of the absorbent carbon material, which can also result in more stable adsorbents [4].

There are many other methods that could be applied for wastewater treatment using the principle of adsorption;

---

\* Corresponding author.

biosorption obtained during the anodic oxidation when anodes are replaced by vegetable material (*Luffa cylindrical*) [5].

Lead represents a common heavy metal present inside wastewaters that cause a lot of risk if it exceeds the permissible limit. According to WHO (World Health Organization), the maxi allowable lead within drinkable waters is 0.1 mg/L [6,7].

Adsorption represents an efficient technique which employed for removing heavy metals from wastewaters, owing to many advantages like several low cost adsorbents, simple, high capacity, and environmentally friendly [8–10].

In recent decades, the emphasis has been placed on the use of agricultural materials to get activated carbon like Almond shell due to its high availability and low preparation costs [11,12].

Adsorbent materials are able to bind heavy metal ions through giving a couple of electrons to create complexes along with metal ions via processes of reacting, through chemisorption, diffusing via pores, complexing as well as absorbing on the surface. Table 1 summarizes some from agricultural materials studied to remove the lead out of a number of aqueous solutions [13]

Table 1  
Agricultural wastes utilized as adsorbent to remove the lead out of aqueous solution [13]

Adsorbent material	Uptake capacity (mg/g)	Maximum removal %
Activated bamboo charcoal	53.76	83.01
Almond	8.08	68
Peels of banana	2.18	85.3
Coconut	4.38	60
Coir	0.127	86.98
Okra waste	5	99
Tea waste	73	96

In northern Iraq, almond trees are cultivated in abundance so there are good quantities from almond shell that may be utilized in a beneficial way such as the production of activated carbons. Several scholars have investigated the use of almond husk in different methods to obtain activated carbon and use it as a sorbent material to remove heavy metals [14–16].

To gain the optimal purpose of any adsorption process, a need arose to employ a high-quality representation model that can explain process performance and how to evolve and predict process behaviour. One of these applications is the artificial neural network (ANN) as it has been used as a powerful tool on a large scale to solve environmental problems due to reliable, robust and can capable dealings complex and non-linear systems [17,18].

As for the present study, the use of activated carbon prepared from Almond shells will be evaluated using a chemical activation method to remove lead (Pb) from contaminated water using the adsorption process. ANN is applied to investigate experimental data for removal efficiency, as well as the use of adsorption isotherms and kinetic modelling to illustrate the procedure of removing lead from contaminated water.

## 2. Material and techniques

### 2.1. Preparing activated carbon

Almond shells were utilized in this study after cleaning and grinding to get a particle size between 2 to 1 mm, then almond shell mixed with a phosphoric acid solution ( $H_3PO_4$ ) (85%) in a weight ratio of (1:1). The carbonization process for the mixture happened in a furnace for 3 h at 550°C. After the chemical activation, carbon was made cool within room temperature and cleaned with (0.2 N) of NaOH (sodium hydroxide) a number of times, after that it was washed with deionized waters till the pH reached 6–7. Finally, drying the activated carbon that was prepared during 3 h at 100°C.

### 2.2. Batch adsorption experiments

Removal of heavy metal lead ion from wastewater used batch adsorption isotherms was investigated via the addition of 0.2, 0.4 and 0.8 g from activated carbon into 100 ml solution with concentrations of  $Pb^{+2}$  5, 10 and 20 mg/l, then mixing and placing in the stirrer for about 120 min. Five studied variables include the initial lead concentration, pH value of the solution adjusted between 4, 7 and 9 by the addition of 0.2 N HCl and 0.2 N NaOH, adsorbent dosage, contact time studied at intervals of 20 min from 0 to 120 min, and stirring the speed that was examined at 30,60 and 90 rpm. The adsorbent was removed by Whatman filter paper before analysing the concentrations of lead via atomic absorbing spectrophotometer. The percentage of the removed metal ions was obtained according to Eq. (1) and the amount of lead adsorbed onto the almond shell activated carbon at equilibrium was measured according to Eq. (2) as shown below: [19]

$$R\% = \frac{C_0 - C_t}{C_0} \times 100\% \quad (1)$$

$$q_e = \frac{C_0 - C_e}{M} V \quad (2)$$

where ( $R\%$ ) is the ratio of removal metal concentration,  $C_0$ ,  $C_t$  and  $C_e$  represent the initial at time  $t$  and equilibrium concentration (mg/L) of lead before as well as after adsorption,  $q_e$  represents the adsorbed lead quantity at equilibrium (mg/g),  $V$  represents the size of lead solution (L), while  $M$  represents the amount of adsorbent (g) [19].

### 2.3. ANN (Artificial neural network) modelling

Artificial neural networks (ANN) are a type of unconventional modeling procedure used to study the performance of a process without knowledge of the system, then classifying, recognizing and predicting data were developed based on a simulation process similar to the biological nervous system of the human brain [20]. The fundamental processing component of ANN was named neurons, which are connected to a network by a group of weights. The basic artificial neural network configuration involves three layers' kinds: the layer of input, hidden and output.

The first layer gathers input variables, manipulates them to the hidden layer, and the output layer provides ANN predicted response. Each layer has a number of neurons connected together. A neuron gets a signal from the input or another neuron, then processes it by weights that represent the power of communicating between two neurons, which are changed by the transferring task to create the output. At that time, the output signal is broadcasted to another neuron until reaching the network's output [21].

The paper used the applicability of the three layer feeding to forward ANN modelling by using a back broadcast algorithm (5:10:1) by employing tansig transferring within the concealed layer and the purelin transferring task within the output layer to predict the removal efficiency of activated carbon out of almond shell for removal Pb(II) ions as shown in Fig. 1. MSE (mean square error) has been utilized as the error task and this measures the network's performance [18].

2.3.1. Sensitivity analysis

Sensitivity analysis or the relative importance of ANN modelling is used to measure the influence of any input variable upon process outcomes. The sensitivity analysis was performed on the basis of the Garson equation and relied on a neural net weight matrix as shown in Eq. (3) [22,23].

$$R = \frac{\sum_{e=1}^{e=H} \left( \frac{|w_{ae}^{ab}|}{\sum_{d=1}^N |w_{ke}^{ab}|} \right) \times |w_{en}^{bc}|}{\sum_{d=1}^{d=N} \left\{ \sum_{e=1}^{e=H} \left( \frac{|w_{ke}^{ab}|}{\sum_{d=1}^N |w_{de}^{ab}|} \right) \times |w_{en}^{bc}| \right\}} \quad (3)$$

where  $R$  is the relative importance of inputs variables upon output variables;  $N$  plus  $H$  represent the figures of input plus

hidden neurons; while  $W$  is a connecting weight; the symbols  $a, b,$  and  $c$  symbolize the layers of input, hidden, and output; finally the symbols  $d, e,$  and  $n$  represent the neurons of input, hidden, and output.

2.4. Adsorption isotherm of lead on activated carbon

Adsorption isotherm was applied to depict the capacity of adsorbent and adsorbing lead conduct on the activated carbon from the almond shell, isotherm represents the relation amid the quantity of lead ion removed via the adsorbents with the ion that remains inside a solution at a constant temperature at equilibrium. In the current work, Langmuir along with Freundlich equations had been utilized to assess equilibrium data. These isotherms were determined by Eqs. (4)–(6) [10,24]:

$$\frac{C_e}{q_e} = \frac{1}{Mq_m} + \frac{C_e}{q_m} \quad (4)$$

$$R_L = \frac{1}{(1 + MC_0)} \quad (5)$$

$$\ln q_e = \ln b + \frac{1}{a} \ln C_e \quad (6)$$

As  $q_e$  represents the quantity of the lead ion absorbed (mg/g),  $C_0$  plus  $C_e$  represent the initial plus equilibrium concentrations of lead ion inside solution (mg/L),  $M$  represents the Langmuir constant (L/mg),  $q_m$  represents the maximum quantity of the adsorption (mg/g), and  $R_L$  designates the isotherm kind to be irreversible its favourable ( $0 < R_L < 1$ ) or unfavorable ( $R_L > 1$ ),  $b$  L/g represents the adsorbent capability while a g/L represents the adsorption intensity of the Freundlich constant. The suitable adsorption happens when the values of  $a$  between ( $1 < a < 10$ ) [10,24]. The adsorption isotherm of Pb(II) on almond shell activated carbon was investigated with different doses of activated

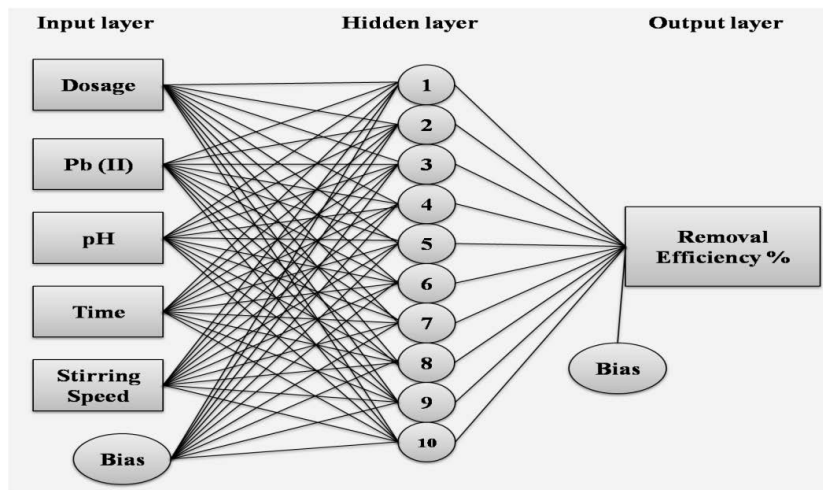


Fig. 1. ANN model architecture.

carbon 0.2, 0.4 and 0.8 g and contact time 120 min at 120 rpm stirring speed, lead concentration 10 mg/L and pH 7.

$$\frac{t}{q_t} = \frac{1}{(k_2 q_e^2)} + \frac{1}{q_e} t \tag{8}$$

2.5. Adsorption kinetics

The adsorbing kinetic of lead ion on activated carbon out of almond shell has been evaluated on the solution containing 10 mg/L of Pb(II) ion with pH 7 and 0.4 g of the adsorbent for contact times ranging from 0 to 100 min. The experimental data were tested by Lagergren modelling and pseudo-second-order kinetics to label the adsorption. The pseudo-first-order equation (Lagergren model) and pseudo-second-order could be stated by Eqs. (7) and (8) as follows: [25,26]

$$\log(q_e - q_t) = \log q_e - \frac{k_1}{2.303} t \tag{7}$$

where  $q_t$  and  $q_e$  represent the adsorbing ability at time  $t$  and equilibrium (mg/g),  $k_1$  refers to the ratio constant of Lagergren model adsorption (l/min) and  $k_2$  (g/mg min) refers to the ratio constant of pseudo-second-order [25].

3. Discussing the results

3.1. Characterization of activated carbon from almond shell

3.1.1. SEM morphology analysing

Fig. 2 shows the SEM (scanning electron microscope) has been utilized to examine the surface morphology of the activated carbon from the almond shell as shown in.

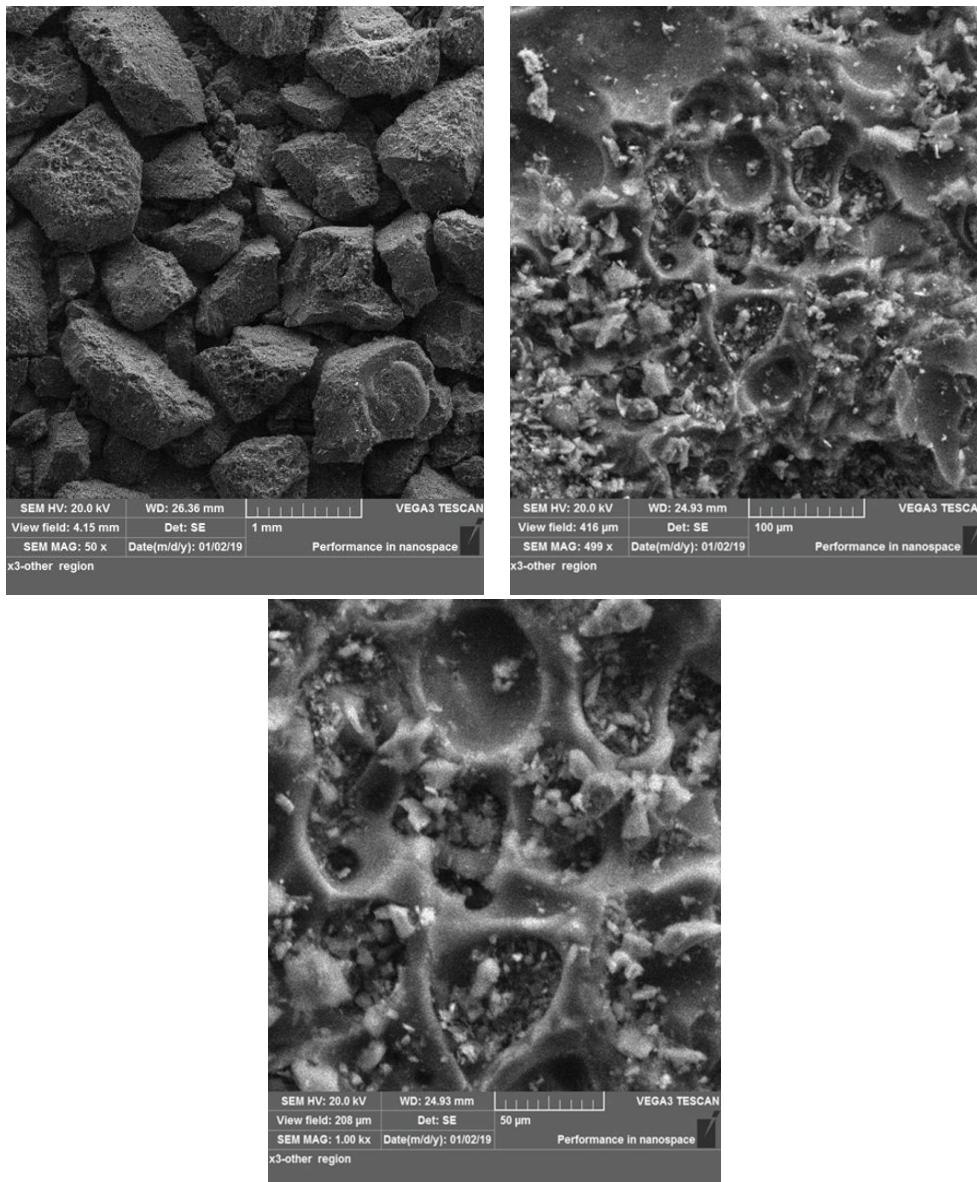


Fig. 2. SEM imaging of almond shell activated carbon.

The activated carbon showed a high porosity structure indicating that the surface areas are approximately elevated with large cracks, channels, and perforations with an average pore diameter equal to 50  $\mu\text{m}$ . This large porosity happens through the carbonization process of almond shells by phosphoric acid at a great temperature (550°C), Phosphoric acid represents a robust dehydration factor which leads to decompose organic materials and to discharge volatile matters and inhibit the formation of tar [16,27]. It observed some tiny white substance dispersed in activated carbon due to  $\text{H}_3\text{PO}_4$  residues through the carbonization procedure.

### 3.1.2. Energy-dispersive X-ray (EDX) analysing

The EDX technique can be utilized for determining the elemental chemical structure of activated carbons [28]. EDX analysis elucidates that the activated carbon from the Almond shell contains four elements (C, O, P and Si) as shown in Fig. 3. The carbon content is high above 74 wt%, which denotes that the activated carbon preparation process was effective, the presence of oxygen and phosphorus because of the usage of a phosphoric acid solution in the carbonization procedure.

### 3.1.3. X-ray diffraction (XRD)

The XRD (Model: XRD 6000 Shimadzu, Japan) was performed with nickel-filtered  $\text{Cu-K}\alpha$  radiation ( $\lambda = 0.154056 \text{ nm}$ ) at a voltage 40 kV and a current 30 mA to determine patterns of activated carbon as shown in Fig. 4. The three broad peaks of activated carbon, corresponding to  $2\theta = 25.5^\circ$ ,  $2\theta = 43.7^\circ$  and  $2\theta = 79.4^\circ$  in the spectrum, were allocated to the 002 plane, 100 plane and 110 plane. The presence of a wide diffracting background and the nonappearance of a shrill peak disclose a principally amorphous construction, and these are similar to the peaks of the graphite structure that corresponds to the data card, it is a special feature to activate carbon (JCPDS Card no.75-1621) [29,30].

The crystal size of almond shell activated carbon got calculated by utilizing the Scherrer Eq. (9) [31,32]

$$L_c = \frac{k\lambda}{\beta \cos\theta} \quad (9)$$

where  $L_c$  represents the average crystallite size (nm),  $\lambda$  is the wavelength of the X-ray radiation ( $\lambda = 0.154056 \text{ nm}$ ),  $K$  is the Scherrer constant ( $K = 0.9$ ),  $\beta$  is FWHM (a full-width at half maximum) of the plane and  $\theta$  represents the Bragg

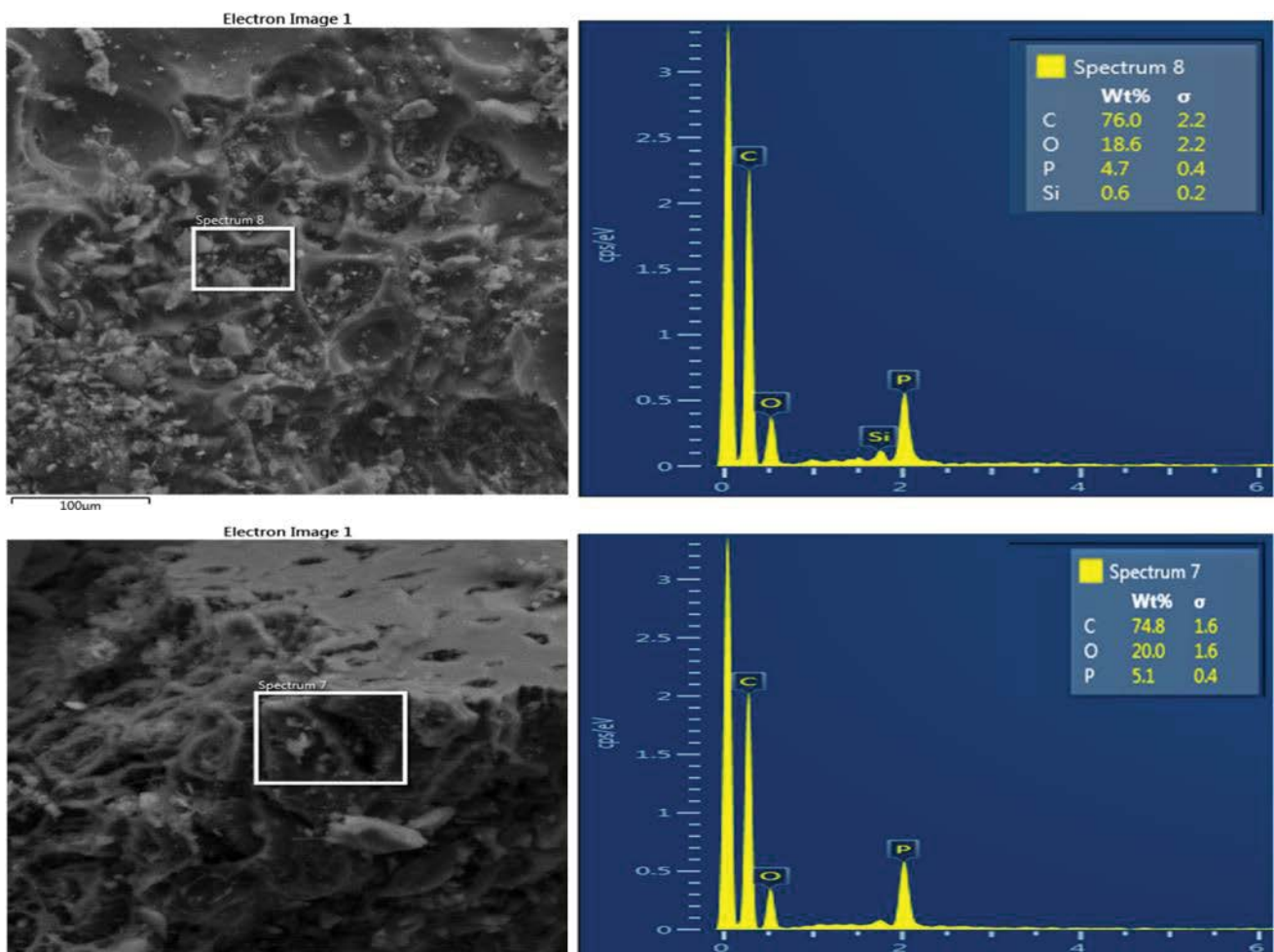


Fig. 3. EDXA spectra of almond shell activated carbon.



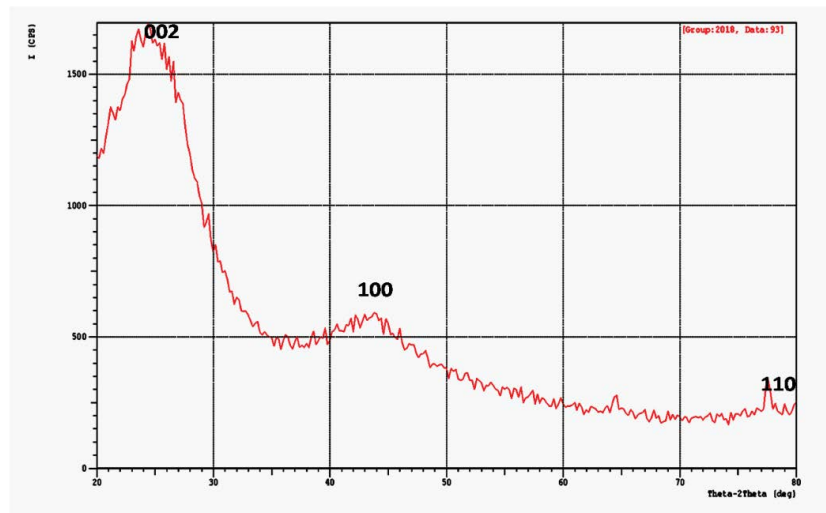


Fig. 4. XRD of almond shell activated carbon.

angle [32]. The parameters extracted from the curve fitting of XRD spectra and particle size are presented in Table 2. From the table, it appears that the average pore size diameter equals to 1.4 nm, it is considered to be a suitable carbon pore size for adsorption.

Table 2

The parameters extracted from the curve fitting of XRD spectra and particle size

hkl	2θ (deg)	1/l	FWHM(rad) (B)	$L_c$ (nm)
002	25.5662	100	0.114193078	1.245066
100	43.7847	25	0.117284233	1.274084
101	79.4187	10	0.107283333	1.679991

### 3.2. Experimental results

An experimental parametric study is carried out to determine the efficiency of activated carbon of almond shell in removing the lead and was compared with predictable data from ANN. Experimental variables for the adsorption process were utilized as input data for a neural network to train and calculate the output removal efficiency of lead. With 10 hidden neurons, the values of MSE and  $R_2$  were 0.0004283 and 0.99658 respectively. Fig. 5 illustrates the plotting of the graphical output of the neural network output against experimental data (targets). The linear regression affirms that the neural network modelling is a suitable method to forecast the experimentation adsorption data.

#### 3.2.1. Effect of pH

The pH of the solution possesses an important influence upon the adsorption characteristics of lead onto the Almond shell activated carbon. The influence of various pH values 4, 7 and 9 on lead adsorption was studied according to the following settings: The time used was 120 min,

Pb(II) concentration of 10 mg/L mixed with 0.4 g of adsorbent, stirring speed 120 rpm and 100 ml of solution was kept constant. Fig. 6 shows a comparison between the predicted and experimental values of removal lead with time. It was observed that at pH 7 maximum removal 100% was obtained due to the electrostatic attracting among the Pb(II) cations within the solution, the negative charge surface of the Almond shell activated carbon and the lowest percent 59% at an acidic pH of 4, the reason behind this is that acidic pH presented the minimum uptake of the metals because of cation competitive influences with hydronium  $H_3O^+$  ion, and at pH 9 was 83.64% when pH turned out to be more basic, the adsorbing drops when the metal hydroxides become precipitous [10,11,33].

#### 3.2.2. Effect of initial metal ion concentration

Different concentrations of lead 5, 10 and 20 mg/L were used with contact time 120 min at 120 rpm stirring speed, pH 7 and 0.4 g of the adsorbent. From Fig. 7, the maximum removal efficiency was 100% when the lead concentration was 5 mg/L reached at 60 min and for 10 and 20 mg/L were 100% at 100 min and 95.16% at 120 min, respectively. It can notice that when reduced concentration of lead, removal time decreased as well as the increased removal of lead this is because of the opportunity to have many active sites on the activated carbon of the almond shell. Highly compatible were found between the experimental data and ANN output.

#### 3.2.3. Effect of adsorbent's dosage

Studying the impact of adsorbent's dose on the removal of lead was done via changing from 0.2 to 0.8 g with the contacting time of 120 min, under the specific conditions (pH of 7, 120 rpm stirring speed and Pb(II) concentration of 10 mg/L). Fig. 8 illustrates that increasing of the almond shell activated carbon dosage increased the removal percentage of metal ions, this is because the increasing of the adsorbent's surface area which led to increase the

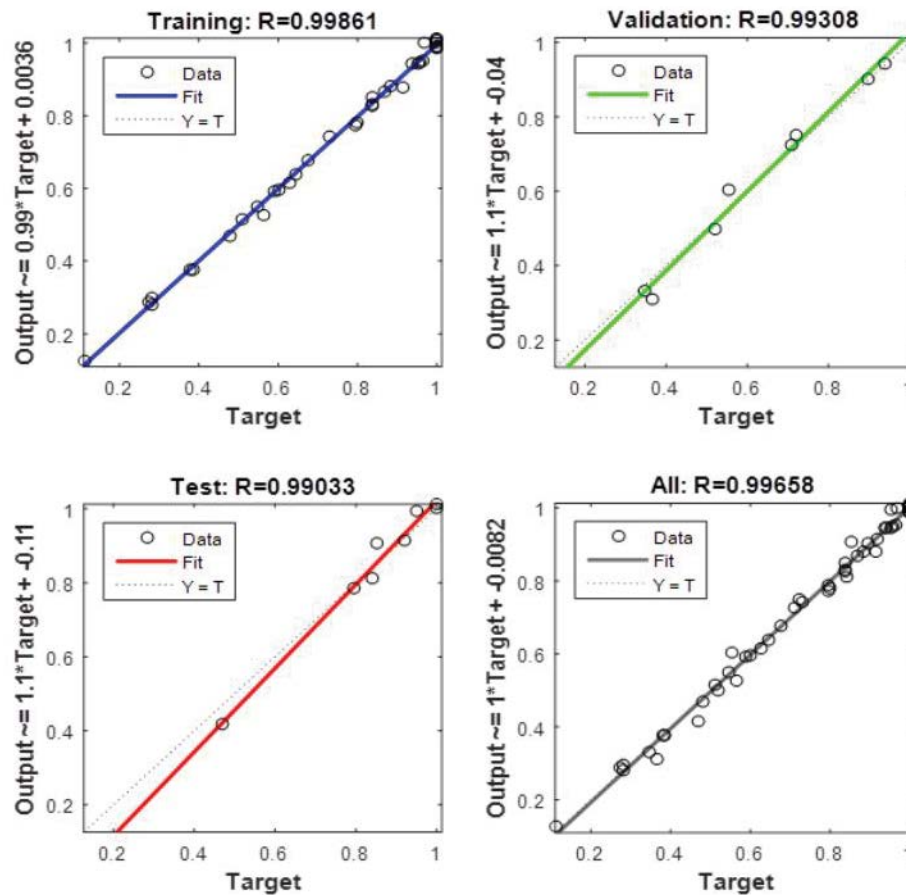


Fig. 5. Target and ANN predicted values.

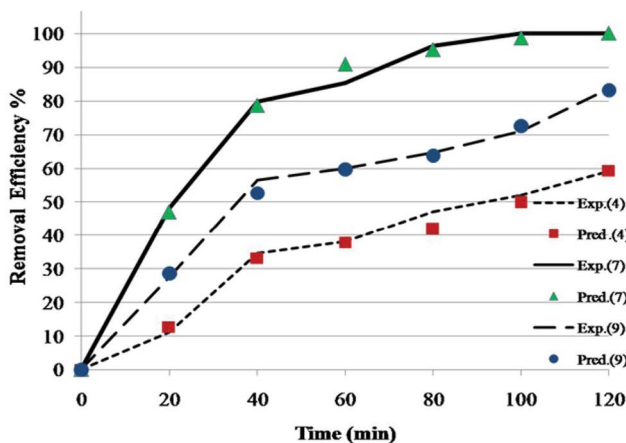


Fig. 6. Influence for pH values on removal efficiency of lead adsorption onto activated carbon from almond shell vs. time (Pb(II) concentration of 10 mg/L, stirring speed 120 rpm and dosage = 0.4 g). Predict and experiment results.

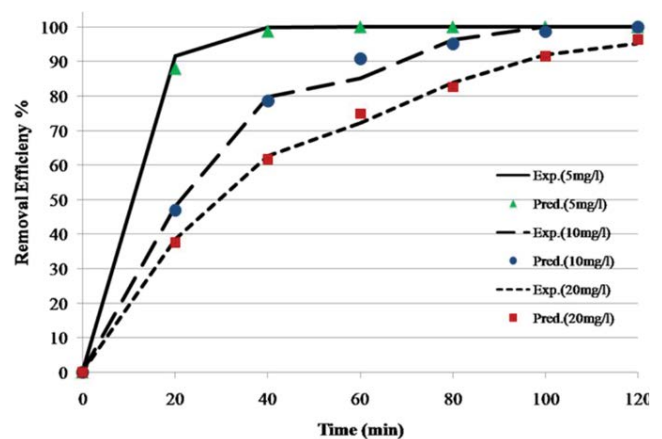


Fig. 7. The influence of various Pb(II) concentrations upon removal efficiency by adsorption onto the activated carbon from almond shell vs. time (stirring speed 120 rpm, pH 7 and dosage = 0.4 g). Predict and experiment results.

active site. The removal of Pb(II) attained maximum removal at an adsorbent dosage of 0.8 g with 100% removal then respectively, for 0.4 and 0.2 g were 96.3% and 80% at time 80 min. Fig. 8 shows the predicted values of ANN model appear to be quite agree with the experimental values.

### 3.2.4. Effect of stirring speed

The investigation of the stirring speed influence was done via using three speeds 30, 60, and 120 rpm under the specified conditions lead ion concentrating of 10 mg/L, contacting time 120 min with pH 7 and 0.4 g of the adsorbent.

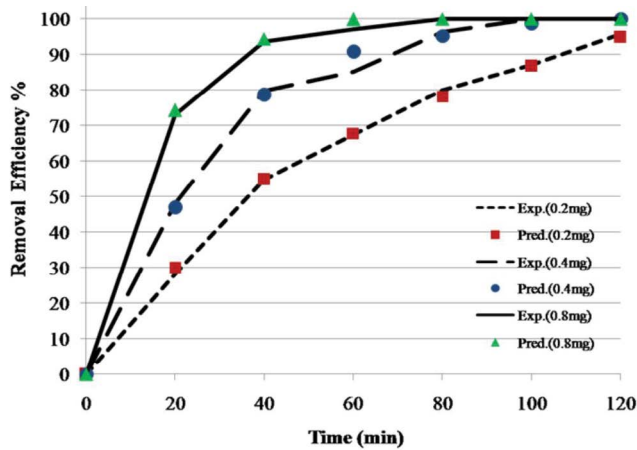


Fig. 8. The effect of different dosages of activated carbon from almond shell on removal efficiency by adsorption vs. time (stirring speed 120 rpm, pH 7, Pb(II) concentration of 10 mg/L and dosage = 0.4 g). Predict and experiment results.

It was observed that stirring speed at 120 rpm gave 100% removal for the lead at the less mixing time of 100 min than other speeds as shown in Fig. 9. Increasing the stirring speed leads to increase in lead removal this because the effect of stirring speed on adsorption by diffusion and when increase turbulence, the rate of diffusion is increased and reach equilibrium faster. Stirring the speed of 60 rpm and 30 rpm gave 100% and 94% removal efficiency at time 120 min, the reason behind this is that with little mixing there is a need for more contacting time to reach the equilibrium. From Fig. 9 it can be that the predicted data from ANN is almost close to the experimental data.

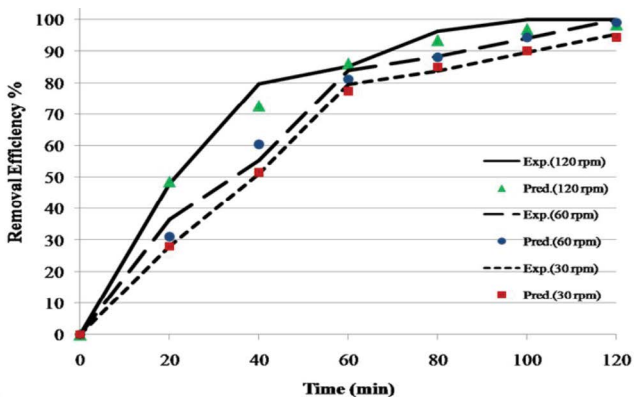


Fig. 9. Effect of stirring speed on removal efficiency of lead adsorption onto activated carbon from almond shell vs. time (pH 7, Pb(II) concentration of 10 mg/L, and dosage = 0.4 g). Predicted and experimental results.

### 3.3. Sensitivity analysis

Studying the influence of each variable upon the adsorbing process was done using sensitivity analysis depending on Eq. (3). Table 3 shows the relative importance of each input variables (Pb(II) concentration, pH, contacting time, stirring speed and dosage of activated carbon). It can see that

Table 3

The relative importance of variables that input in the adsorption process

Input variables	Relative importance %
Activated carbon	28.6
pH	22.2
Pb(II) concentration	21
Time	19.5
Stirring speed	8.7

activated carbon dosage was the most important among the variables and the lowest was stirring speed.

### 3.4. Adsorption isotherm

Fig. 10 shows langmuir and freundlich adsorption isotherms of Pb(II) onto the activated carbon from the almond shell. Table 4 presents information about the parameter values and the correlation coefficient of isotherm models. Correlation coefficient ( $R^2$ ) of freundlich was 0.981 and for langmuir was 0.933, this is evidence that isotherm freundlich is the best and closest to explaining the state of adsorption which tends to be heterogeneous and multi layered. In the current work, the value was equal to 2.3923 g/L that is greater than 1, so spontaneous adsorption occurs in this process.

Table 4

Adsorption isotherm parameters for Pb(II) adsorption onto the almond shell activated carbon

Adsorption isotherm	Parameter	Almond shell activated carbon
Langmuir	$q_m$ (mg/g)	4.31
	$M$ (L/mg)	0.928
	$R_L$	0.0973
	$R^2$	0.933
Freundlich	$b$ (L/g)	1.954
	$a$ (g/L)	2.3923
	$R^2$	0.981

### 3.5. Adsorption kinetics

Fig. 11 displays the adsorption kinetics of the lead ion on the almond shell activated carbon and Table 5 exhibits the kinetic parameters for the two models used. Depending on the correlating constant, pseudo-second-order ( $R^2 = 0.988$ ) gave the best description of the kinetic demeanour of the process when compared with the Lagergren model ( $R^2 = 0.946$ ), therefore the process tends to be chemisorptions is most likely the ratio-limit step which has control on the overall adsorbing procedure. It was found that the pseudo-second-order modelling is the best suitable modelling to signify the current data [34].

Generally, the electrochemical relation between AC prepared from various materials and pollutants considered to be the governing factor that control pollutants diffusion through pores [35].



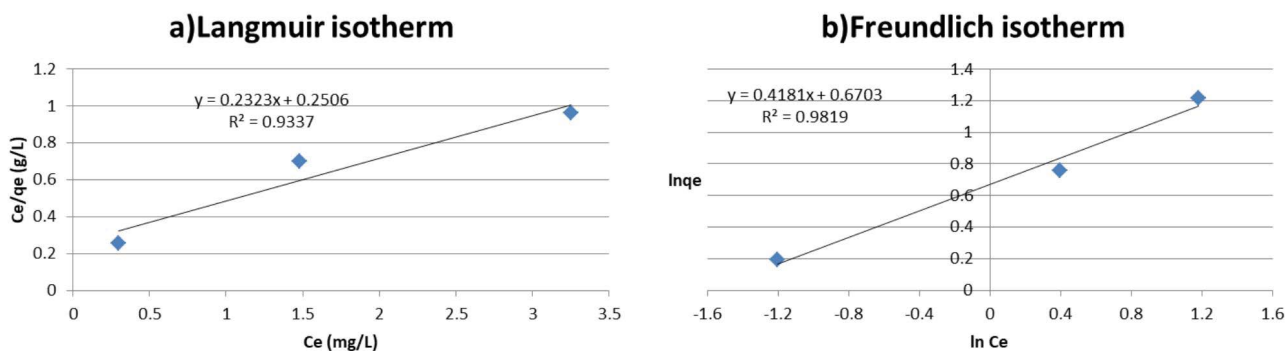


Fig. 10. Isotherm models (a) Langmuir and (b) Freundlich.

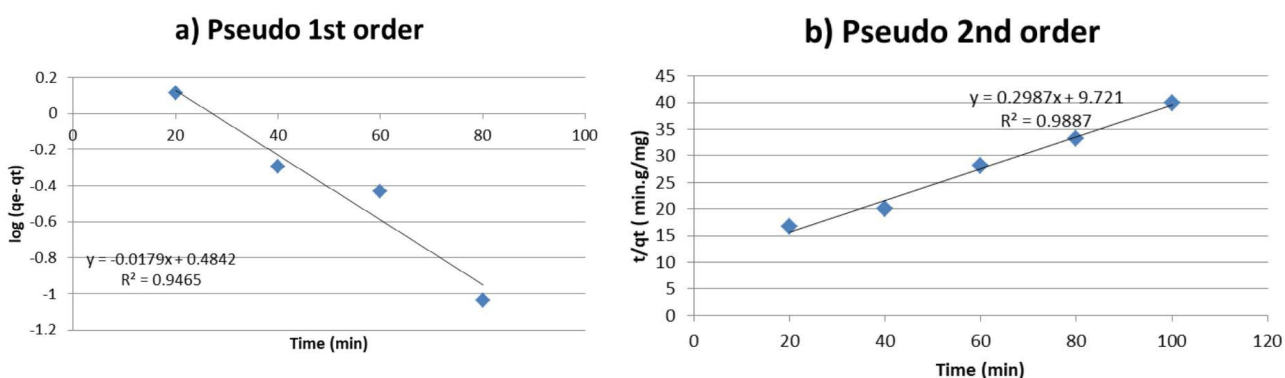


Fig. 11. Kinetics model (a) pseudo-first-order and (b) pseudo-second-order.

Table 5  
Adsorbing kinetic parameters for Pb(II) adsorbing onto the almond shell activated carbon

Model	Parameter	Almond shell activated carbon
Pseudo-first-order	$q_e$ (mg/g)	3.0479
	$K_1$ (l/min)	0.039151
	$R^2$	0.946
Pseudo-second-order	$q_e$ (mg/g)	2.712
	$K_2$ (g/mg min)	0.009135
Experimental	$R^2$	0.988
	$q_e$ (mg/g)	2.5

#### 4. Conclusion

The current work confirmed that activated carbon made by almond shell in weight ratio 1:1 of 85%  $H_3PO_4$  at 550°C for 3 h can remove lead ion from contaminated water using a batch adsorbing process. A three-layer feed forward ANN modelling that applied to investigate the removing effectiveness of lead gave impressive results through estimate and predict data with MSE and  $R^2$  were 0.0004283 and 0.99658 respectively. The impact of experimental variables employed on the adsorption process were studied by relative importance and showed that the activated carbon dose was the most important among the others, this was proved

by using ANN model. The isotherm freundlich model was the closest to explain the state of adsorption which tends to be heterogeneous and multi layered. The pseudo-second-order gave the finest explanation of the kinetic demeanor of the process, therefore, the process tends to be chemisorption. The mechanism governing Pb(II) adsorption is controlled by diffusion in AC pores.

#### References

- [1] M.P. Aji, P.A. Wiguna, J. Karunawan, A.L. Wati, Removal of heavy metal nickel-ions from wastewaters using carbon nanodots from frying oil, *Procedia Eng.*, 170 (2017) 36–40.
- [2] N.M. Hilal, I.A. Ahmed, R.E. El-Sayed, Activated and non-activated date pits adsorbent for the removal of copper(II) and cadmium(II) from wastewater, *ISRN Phys. Chem.*, 2012 (2012) 985853, doi: 10.5402/2012/985853.
- [3] A. Othmani, J. John, H. Rajendran, A. Mansouri, M. Sillanpää, P.V. Chellam, Biochar and activated carbon derivatives of lignocellulosic fibers towards adsorptive removal of pollutants from aqueous systems: critical study and future insight, *Sep. Purif. Technol.*, 274 (2021) 119062, doi: 10.1016/j.seppur.2021.119062.
- [4] Z.U. Zango, N.S. Sambudi, K. Jumbri, A. Ramli, N.H.H. Abu Bakar, B. Saad, M.N.H. Rozaini, H.A. Isiyaka, A.M. Osman, A. Sulieman, An overview and evaluation of highly porous adsorbent materials for polycyclic aromatic hydrocarbons and phenols removal from wastewater, *Water*, 12 (2020) 2921, doi: 10.3390/w1210292.
- [5] A. Othmani, A. Kesraoui, H. Akrouf, I. Elaissaoui, M. Seffen, Coupling anodic oxidation, biosorption and alternating current as alternative for wastewater purification, *Chemosphere*, 249 (2020) 126480, doi: 10.1016/j.chemosphere.2020.126480.

- [6] A.A. Mengistie, T. Siva Rao, A.V. Prasada Rao, M. Singanan, Removal of lead(II) ions from aqueous solutions using activated carbon from *Militia ferruginea* plant leaves, *Bull. Chem. Soc. Ethiop.*, 22 (2008) 349–360.
- [7] H.Z. Mousavi, A. Hosseynifar, V. Jahed, S.A.M. Dehghani, Removal of lead from aqueous, *Braz. J. Chem. Eng.*, 27 (2010) 79–87.
- [8] A.A. Alghamdi, A.-B. Al-Odayni, W.S. Saeed, A. Al-Kahtani, F.A. Alharthi, T. Aouak, Efficient adsorption of lead(II) from aqueous phase solutions using polypyrrole-based activated carbon, *Materials (Basel)*, 12 (2020), doi: 10.3390/ma12122020.
- [9] J.H. Al-Baidhani, S.T. Al-Salihy, Removal of heavy metals from aqueous solution by using low cost rice husk in batch and continuous fluidized experiments, *Int. J. Chem. Eng. Appl.*, 7 (2016) 6–10.
- [10] K. Manzoor, M. Ahmad, S. Ahmad, S. Ikram, Removal of Pb(II) and Cd(II) from wastewater using arginine cross-linked chitosan-carboxymethyl cellulose beads as green adsorbent, *RSC Adv.*, 9 (2019) 7890–7902.
- [11] S. Dowlatshahi, A.R.H. Torbati, M. Loei, Adsorption of copper, lead and cadmium from aqueous solutions by activated carbon prepared from saffron leaves, *Environ. Health Eng. Manage. J.*, 1 (2014) 37–44.
- [12] H. Ben Amor, A. Mabrouk, N. Talmoudi, Preparation of activated carbon from date stones: optimization on removal of indigo carmine from aqueous solution using a two-level full factorial design, *Int. J. Eng. Res. General Sci.*, 3 (2015) 6–17.
- [13] A. Kaushal, S.K. Singh Adsorption phenomenon and its application in removal of lead from waste water: a review, *Int. J. Hydrol.*, 1 (2017) 38–47.
- [14] I. Bhatti, K. Qureshi, R.A. Kazi, A.K. Ansari, Preparation and characterisation of chemically activated almond shells by optimization of adsorption parameters for removal of Cr(VI) from aqueous solutions, *Int. J. Chem. Biomol. Eng.*, 1 (2007) 199–204.
- [15] S. Yildiz, Kinetic and isotherm analysis of Cu(II) adsorption onto almond shell (*Prunus Dulcis*), *Ecol. Chem. Eng. S*, 24 (2017) 87–106.
- [16] P.K. Chayande, S.P. Singh, M.K.N. Yenkie, Characterization of activated carbon prepared from almond shells for scavenging phenolic pollutants, *Chem. Sci. Trans.*, 2 (2013) 835–840.
- [17] A. Kardam, K.R. Raj, J.K. Arora, M.M. Srivastava, S. Srivastava, Artificial neural network modeling for sorption of cadmium from aqueous system by shelled *Moringa oleifera* seed powder as an agricultural waste, *J. Water Resour. Prot.*, 2 (2010) 339–344.
- [18] D. Sarala Thambavani, B. Kavitha, Prediction and simulation of chromium(VI) ions removal efficiency by riverbed sand adsorbent using Artificial Neural Networks, *Int. J. Eng. Sci. Res. Technol.*, 3 (2014) 906–913.
- [19] Z. Yi, J. Yao, M. Zhu, H. Chen, F. Wang, X. Liu, Kinetics, equilibrium, and thermodynamics investigation on the adsorption of lead(II) by coal-based activated carbon, *SpringerPlus*, 5 (2016) 1–12.
- [20] S.C.G. Moraes, L.E.M.C. Zaidan, D.C. Napoleão, F.O. Carvalho, M.C.B. Montenegro, V.L. Da Silva, Implementing artificial neural networks modelling after the treatment of oil refinery effluents using advanced oxidation processes, *Braz. J. Pet. Gas*, 10 (2016) 23–32.
- [21] S.L. Pandharipande, A.R. Deshmukh, Artificial neural network approach for modeling of adsorption of Ni(II) and Cr(VI) ions simultaneously present in aqueous solution, *Int. J. Adv. Eng. Technol.*, 6 (2013) 114–127.
- [22] H.M. Madhloom, A.H. Khalil, Z.T. Abd Ali, Artificial neural network for modeling of Cu(II) bio-sorption from simulated wastewater by fungal biomass, *J. Eng. Dev.*, 19 (2015) 210–222.
- [23] Y.A. Mustafa, G.M. Jaid, A.I. Alwared, M. Ebrahim, The use of artificial neural network (ANN) for the prediction and simulation of oil degradation in wastewater by AOP, *Environ. Sci. Pollut. Res.*, 21 (2014) 7530–7537.
- [24] N.M. Mahmoodi, J. Abdi, D. Bastani, Direct dyes removal using modified magnetic ferrite nanoparticle, *J. Environ. Health Sci. Eng.*, 12 (2014) 1–10.
- [25] O. Abdelwahab, Kinetic and isotherm studies of copper(II) removal from wastewater using various adsorbents, *Egypt. J. Aquat. Res.*, 33 (2007) 125–142.
- [26] O.A. Habeeb, R. Kanthasamy, G.A.M. Ali, R.M. Yunus, Isothermal modelling based experimental study of dissolved hydrogen sulfide adsorption from waste water using eggshell based activated carbon, *Malaysian J. Anal. Sci.*, 21 (2017) 334–345.
- [27] K. Li, H. Chen, H. Yu, H. Zhu, Q. Mao, X. Ma, Z. Zhao, T. Xiao, Study on the comprehensive utilization of bitter almond shell, *BioResources*, 9 (2014) 4993–5006.
- [28] D.T. Mekonnen, E. Alemayehu, B. Lennartz, Removal of phosphate ions from aqueous solutions by adsorption onto leftover coal, *Water*, 12 (2020) 1381, doi: 10.3390/w12051381.
- [29] H. Qin, Y. Zhou, J. Huang, C. Zhang, B. Wang, S. Jin, Q. Zhou, Catalytic graphitization strategy for the synthesis of graphitic carbon nanocages and electrochemical performance, *Int. J. Electrochem. Sci.*, 12 (2017) 10599–10604.
- [30] A. Raja, K. Selvakumar, S. Asath Bahadur, S. Asath Bahadur, Photocatalytic degradation of organic pollutant using reduced graphene oxide, *Int. J. Recent Technol. Eng.*, 8 (2019) 870–872.
- [31] P. Scherrer, Göttinger Nachrichten Gesell, Determination of the size and internal structure of colloidal particles by means of X-rays, *Mathematical-Physics Class*, 2 (1918) 98. Available at: <http://www.digizeitschriften.de/dms/resolveppn/?PID=PPN252457811>
- [32] N. Yusof, D. Rana, A.F. Ismail, T. Matsuura, Microstructure of polyacrylonitrile-based activated carbon fibers prepared from solvent-free coagulation process, *J. Appl. Res. Technol.*, 14 (2016) 54–61.
- [33] N.A. Medellin-Castillo, E. Padilla-Ortega, M.C. Regules-Martínez, R. Leyva-Ramos, R. Ocampo-Pérez, C. Carranza-Alvarez, Single and competitive adsorption of Cd(II) and Pb(II) ions from aqueous solutions onto industrial chili seeds (*Capsicum annum*) waste, *Sustainable Environ. Res.*, 27 (2017) 61–69.
- [34] H.H. Abdel Ghafar, G.A.M. Ali, O.A. Fouad, S.A. Makhlof, Enhancement of adsorption efficiency of methylene blue on  $\text{Co}_3\text{O}_4/\text{SiO}_2$  nanocomposite, *Desal. Water Treat.*, 53 (2013) 2980–2989.
- [35] G.A.M. Ali, O. Habeeb, H. Algarni, K.F. Chong, CaO impregnated highly porous honeycomb activated carbon from agriculture waste symmetrical supercapacitor study, *J. Mater. Sci.*, 54 (2019) 683–692.